Cancer Cell
Article

Bronchial and Peripheral Murine Lung Carcinomas Induced by T790M-L858R Mutant EGFR Respond to HKI-272 and Rapamycin Combination Therapy

Danan Li,[1,2,12] Takeshi Shimamura,[1,8,12] Hongbin Ji,[1,2,12] Liang Chen,[1,2] Henry J. Haringsma,[1] Kate McNamara,[1,2] Mei-Chih Liang,[1,2] Samanthi A. Perera,[1,2] Sara Zaghlul,[1,2] Christa L. Borgman,[1] Shigeto Kubo,[3] Masaya Takahashi,[3] Yanping Sun,[4] Lucian R. Chirieac,[5] Robert F. Padera,[5] Neal I. Lindeman,[5] Pasi A. Jänne,[1,8] Roman K. Thomas,[9,10] Matthew L. Meyerson,[1,11] Michael J. Eck,[6] Jeffrey A. Engelman,[7] Geoffrey I. Shapiro,[1,8,13,*] and Kwok-Kin Wong[1,8,13,*]

[1] Department of Medical Oncology, Dana-Farber Cancer Institute, Boston, MA 02115, USA
[2] Ludwig Center at Dana-Farber/Harvard Cancer Center, Boston, MA 02115, USA
[3] Department of Radiology, Beth Israel Deaconess Medical Center, Boston, MA 02115, USA
[4] Department of Radiology
[5] Department of Pathology
Brigham and Women's Hospital, Boston, MA 02115, USA
[6] Department of Cancer Biology, Dana-Farber Cancer Institute, Boston, MA 02115, USA
[7] Department of Medicine, Massachusetts General Hospital and Harvard Medical School, Boston, MA 02129, USA
[8] Department of Medicine, Brigham and Women's Hospital and Harvard Medical School, Boston, MA 02115, USA
[9] Max-Planck-Institute for Neurological Research with Klaus-Joachim-Zülch-Laboratories of the Max Planck Society and the Faculty of Medicine of the University of Cologne, Cologne 50931, Germany
[10] Center for Integrated Oncology, University of Cologne, Cologne 50931, Germany
[11] The Broad Institute of Harvard and Massachusetts Institute of Technology, Cambridge, MA 02141, USA
[12] These authors contributed equally to this work.
[13] These authors contributed equally to this work.
*Correspondence: geoffrey_shapiro@dfci.harvard.edu (G.I.S.), kwong1@partners.org (K.-K.W.)
DOI 10.1016/j.ccr.2007.06.005

SUMMARY

The *EGFR T790M* mutation has been identified in tumors from lung cancer patients that eventually develop resistance to erlotinib. In this study, we generated a mouse model with doxycycline-inducible expression of a mutant *EGFR* containing both L858R, an erlotinib-sensitizing mutation, and the T790M resistance mutation (*EGFR TL*). Expression of *EGFR TL* led to development of peripheral adenocarcinomas with bronchioloalveolar features in alveoli as well as papillary adenocarcinomas in bronchioles. Treatment with an irreversible EGFR tyrosine kinase inhibitor (TKI), HKI-272, shrunk only peripheral tumors but not bronchial tumors. However, the combination of HKI-272 and rapamycin resulted in significant regression of both types of lung tumors. This combination therapy may potentially benefit lung cancer patients with the *EGFR T790M* mutation.

INTRODUCTION

EGFR is a member of the ErbB receptor tyrosine kinase family that also includes HER2/ErbB2/neu, HER3/ErbB3, and HER4/ErbB4. Point mutations and deletion mutations in the kinase domain of *EGFR* have been found to correlate with response to the reversible TKIs gefitinib and erlotinib (Pao et al., 2005). Most *EGFR* mutations fall into four

SIGNIFICANCE

The secondary mutation T790M in the *EGFR* kinase domain is associated with acquired resistance to erlotinib in patients with non-small-cell lung cancer (NSCLC). We demonstrate that expression of an *EGFR* mutant with a T790M-L858R compound mutation in the kinase domain is oncogenic in a mouse model and is essential for tumor maintenance. Combination treatment with the dual-specificity EGFR/ErbB2 irreversible inhibitor HKI-272 and rapamycin induced dramatic tumor regression in these erlotinib-resistant mouse lung cancers, whereas rapamycin or HKI-272 alone failed to produce significant responses. Our findings uncover a potential limitation of irreversible TKI therapy against lung cancers harboring *EGFR TL* and offer an alternative therapeutic strategy for NSCLC patients who eventually develop erlotinib resistance.

major classes: single-base substitutions in exon 18; deletions in exon 19; insertion/duplications in exon 20; and a single-base substitution, L858R, in exon 21 (Shigematsu and Gazdar, 2006). ErbB2 is a favored heterodimerization partner for EGFR and may be expressed at high levels in NSCLC, in some cases as a result of gene amplification. Both EGFR and ErbB2 transphosphorylate ErbB3, which controls PI3K survival signaling in ErbB-driven cancers (Engelman and Cantley, 2006).

Although large phase III trials have shown that erlotinib prolongs survival (Shepherd et al., 2005), patients who initially respond to this TKI almost invariably develop drug resistance. It is estimated that approximately 50% of acquired erlotinib resistance is due to the emergence of a secondary mutation, T790M, in the kinase domain of *EGFR* (Johnson et al., 2006; Riely et al., 2006). Structural analyses suggest that the T790M mutation appears to sterically hinder the binding of erlotinib to the EGFR kinase domain by introduction of a bulky methionine residue, thereby conferring resistance to the drug (Kobayashi et al., 2005a; Pao et al., 2005). Of note, a recent study identified the EGFR T790M mutation as a germline allele in a lung-cancer-prone family, suggesting that this mutation alone may harbor oncogenic potential (Bell et al., 2005).

In order to overcome resistance conferred by the *EGFR T790M* mutation, the use of irreversible dual-specificity EGFR/ErbB2 inhibitors has been proposed (Kobayashi et al., 2005b). HKI-272 belongs to this class of inhibitors and is one of the first in clinical trials. In vitro studies have shown that HKI-272 is an effective inhibitor of the EGFR T790M mutation (Kwak et al., 2005). Additionally, we have previously shown that HKI-272 has similar or better efficacy than erlotinib in treating activating *EGFR* kinase domain mutant- and *EGFR*vIII-driven mouse lung adenocarcinomas (Ji et al., 2006a, 2006b). However, it remains unknown if this class of ErbB family inhibitors will effectively treat human lung cancers harboring the *EGFR T790M* mutation.

Mounting evidence suggests that the PI3K/Akt/mTOR pathway plays a pivotal role in tumorigenesis and tumor maintenance (Engelman et al., 2005). Activated mTOR signaling, defined by expression of phospho-S6 in tumor tissue, has been associated with *EGFR* mutant lung cancers (Conde et al., 2006). mTOR integrates signals from both growth factor and nutrient transduction pathways (Vogt, 2001) and is critical for ribosome biogenesis and cell growth (Hay and Sonenberg, 2004). However, rapamycin analogs have shown limited efficacy in clinical trials (Vignot et al., 2005). This may be partially due to the abrogation of mTOR-S6-dependent feedback inhibition of both insulin-like growth factor receptor substrate-1 (IRS-1) and PI3K/Akt signaling (Manning, 2004; O'Reilly et al., 2006). Rapamycin may also inhibit mTOR-S6-mediated negative feedback of other growth factor receptors as well (Hay, 2005).

To evaluate the biological function of the compound EGFR TL mutation in lung tumorigenesis and its sensitivity to TKIs, we generated a doxycycline-inducible bitransgenic mouse model that expresses *EGFR TL*. Our data reveal that lung-specific expression of *EGFR TL* leads to development of lung adenocarcinomas that are dependent on EGFR signaling for their continued survival. *EGFR TL*-driven tumors are resistant to erlotinib but show dramatic response to HKI-272 and rapamycin combination therapy, suggesting that suppression of both EGFR activation and downstream PI3K-mTOR signaling is important for the efficacy of this therapeutic strategy.

RESULTS

Generation of the *Tet-op-EGFR TL/CCSP-rtTA* Mouse Cohort

To generate mice with inducible expression of the human *EGFR TL* compound mutant, we constructed a 4.7 kb DNA segment consisting of seven direct repeats of the tetracycline (tet)-operator sequence, followed by *EGFR TL* cDNA and *β-globin* polyA (Figure 1A and Experimental Procedures). The construct was injected into FVB/N blastocysts, and progeny were screened using a PCR strategy (data not shown). Fifteen *Tet-op-EGFR TL* founders were identified and then crossed to *CCSP-rtTA* mice, an allele that has been shown to specifically target the expression of the reverse tetracycline transactivator protein (rtTA) in type II alveolar epithelial cells, to generate inducible bitransgenic mouse cohorts harboring both the activator and the responder transgenes (Fisher et al., 2001). Four tightly regulated *EGFR TL* founders (#17, #19, #24, and #29) were identified by RT-PCR (Figure 1B). The gene copy number from individual founders was determined by quantitative real-time PCR (Figure 1C).

Tightly Regulated Expression of *EGFR TL* mRNA in Lung Tissue

The inducibility of transgene expression in the lung compartment was evaluated at the RNA level by RT-PCR. The lungs of the bitransgenic mouse *Tet-op-EGFR TL/CCSP-rtTA* cohort for each potential founder were collected before and after 8 weeks of doxycycline administration and after 3 days of doxycycline withdrawal following doxycycline administration over an 8 week period. The *EGFR* mutant transcript was undetectable from either nontransgenic mice or the bitransgenic mice without doxycycline treatment, while it became readily detectable after 8 weeks of doxycycline administration; transcription of mutant *EGFR* was completely abolished by 3 days of doxycycline withdrawal in all of the lines (Figure 1B and data not shown). To further confirm that mutant *EGFR* transcripts are inducible and tightly regulated by doxycycline, both RT-PCR and quantitative real-time PCR were performed on lung samples collected at serial time points of doxycycline administration and withdrawal from founder #19. Mutant *EGFR* expression was observed after 1 week of doxycycline administration and was kept at a comparable level throughout the 8 week period of administration (Figure 1D). Doxycycline withdrawal was sufficient to block the expression of mutant *EGFR*, and no expression of the transgene was observed after 12 weeks of doxycycline withdrawal (Figure 1D).

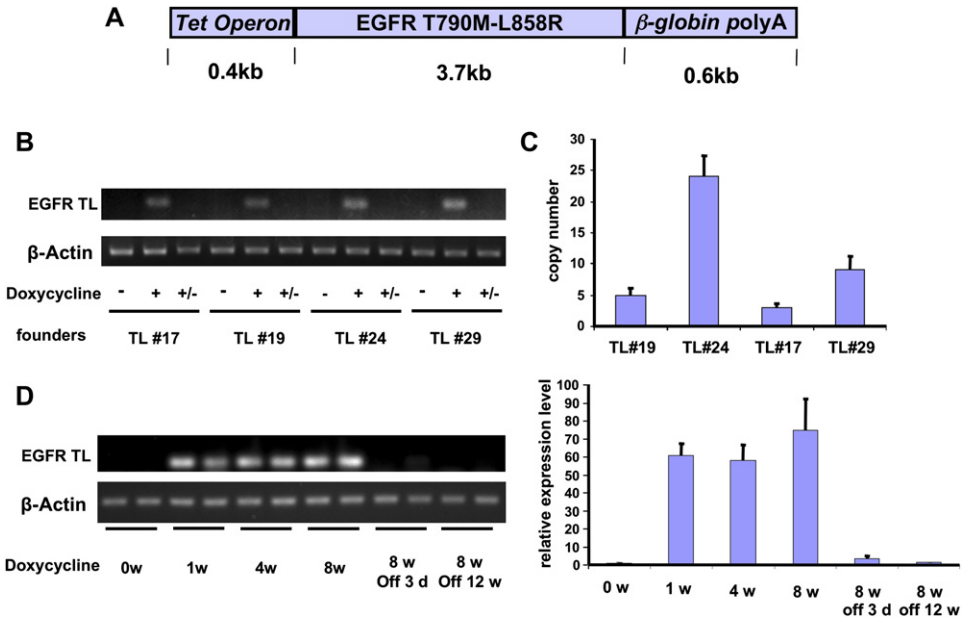

Figure 1. Generation and Characterization of the Bitransgenic Mice with Inducible Expression of *EGFR TL* in Lung Compartments

(A) Scheme of the *EGFR TL* construct for the conditional transgenic mice.

(B) RT-PCR analysis of regulatable expression of *EGFR TL* in lungs of bitransgenic mice derived from four founders. −, on regular food; +, on doxycycline food for 8 weeks; +/−, on doxycycline food for 8 weeks followed by 3 days of regular food.

(C) *EGFR TL* copy number for each founder line. Copy numbers were determined by real-time PCR using tail DNA. Means (columns) and standard deviations (SD; bars) shown were from triplicate experiments.

(D) Time course analysis of EGFR TL expression in founder #19. Expression level was evaluated by regular RT-PCR (left panel) and real-time PCR (right panel) at different time points after indicated doxycycline treatment. Triplicate experiments were performed for each sample.

Overexpression of the *EGFR TL* Mutant Drives the Development of Two Distinct Types of Lung Adenocarcinomas

To determine if overexpression of the *EGFR* mutant would drive lung tumorigenesis, bitransgenic *Tet-op-EGFR TL/CCSP-rtTA* mice on continuous doxycycline administration underwent serial magnetic resonance imaging (MRI) and were sacrificed at various time points for histological examination of the lungs. Tumors could be observed by MRI after 5–6 weeks of doxycycline administration, and tumor volume, as defined by MRI, increased following prolonged doxycycline treatment (Figure 2A, top row). In contrast to untreated mice, lung histology demonstrated the development of early lesions in alveoli after 2–3 weeks of doxycycline treatment. After 4–5 weeks, typical bronchioloalveolar carcinoma (BAC) appeared. Invasive peripheral adenocarcinomas with bronchioloalveolar features appeared after 7–9 weeks and become the dominant histological pattern after 12 weeks of doxycycline treatment (Figure 2A, middle row). The lung peripheral adenocarcinomas observed are histologically similar to those that develop in the *EGFR L858R* mouse model described previously (Ji et al., 2006a; Politi et al., 2006) and are also similar to a subset of erlotinib-sensitive NSCLC occurring in patients.

In addition to peripheral adenocarcinomas, *Tet-op-EGFR TL/CCSP-rtTA* mice also developed bronchial papillary adenocarcinomas. Early papillary neoplasias in the bronchioles were observed after 2–3 weeks of continuous doxycycline administration. These lesions subsequently progressed into adenocarcinomas after an additional 6–8 weeks (Figure 2A, bottom row). Bronchial papillary tumors were found in all of the four identified founders of *Tet-op-EGFR TL/CCSP-rtTA* mice but were absent in all three *EGFR L858R* founders (Figure 2B).

All of the four *Tet-op-EGFR TL/CCSP-rtTA* founders showed similar morphologic features and a similar latency in tumorigenesis (representative photos shown in Figure 2A were from founder #19). In addition, metastatic foci of adenocarcinomas were occasionally observed in lymph nodes of the mice harboring *EGFR TL*-driven lung tumors but not in mice harboring *EGFR L858R*-driven tumors.

Immunohistochemical (IHC) staining for both peripheral and bronchial tumors with prosurfactant protein C (SPC), a unique biomarker for type II pneumocytes in the alveoli, and Clara cell secretory protein (CCSP), a specific marker for Clara cells in bronchiolar epithelium, demonstrated different patterns of differentiation. The majority of peripheral tumors showed intensive SPC staining, implying a type II pneumocyte origin, as expected. In contrast, the bronchial tumors were completely negative for SPC. Interestingly, only a small subset of bronchial tumor cells were positive for CCSP (Figure 3D). It is possible that these tumors are of Clara cell origin, followed by compromised differentiation leading to loss of the CCSP expression marker.

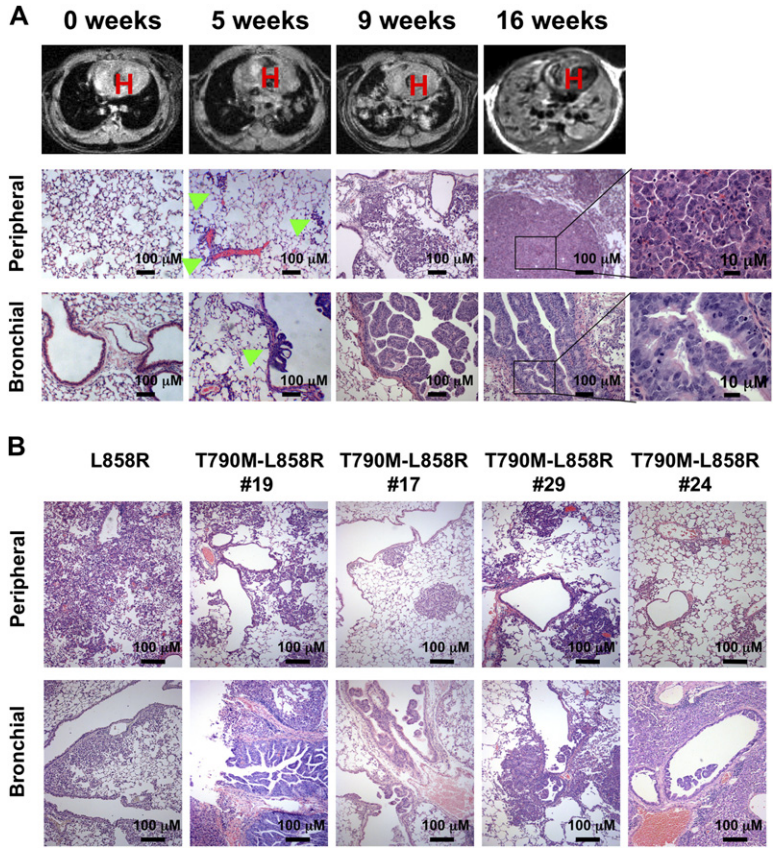

Figure 2. Expression of *EGFR TL* Induces Adenocarcinomas with BAC Features in Alveoli and Papillary Adenocarcinomas in the Bronchioles

(A) Time course analysis of lung tumorigenesis in alveoli and bronchioles after doxycycline administration using both MRI and histology inspection. MRI photographs show increased tumor volume with time of doxycycline administration (top row; H, heart area). Hematoxylin and eosin (H&E)-stained lung sections from the same mice shown in the top row reveal both adenocarcinomas in alveoli and also papillary adenocarcinomas in bronchioles (middle and bottom rows, respectively; arrows, early neoplastic lesions). Photos show representative tumor lesions in the lungs representing average tumor burden among doxycycline-treated mice but not the most severe lesions at particular time point, as emphasized in the text.

(B) Histological comparison between the murine lung tumors with *EGFR L858R* mutation and *EGFR TL* mutation (from all four founders). Note that papillary bronchial tumors were not seen in EGFR L858R mice but observed in all of *EGFR TL* founders. The photographs from founders #19 and #24 also show obstructive pneumonia in addition to bronchial tumors (bottom row).

Expression of the *EGFR TL* Mutant Is Essential for Tumor Maintenance of Both Peripheral and Bronchial Adenocarcinomas

Both peripheral and bronchial lung adenocarcinomas from *EGFR TL/CCSP-rtTA* mice stained positively for total and phospho-EGFR antibodies (Figure 3A, Figure S1 in the Supplemental Data available with this article online, and data not shown), indicating that the expressed EGFR mutant is functionally active. After 3 days of doxycycline withdrawal, no staining with either antibody was observed (Figure 3A and data not shown), implying that both types of tumors are driven by and dependent on EGFR TL for their survival. We also observed an increase in terminal deoxynucleotidyltransferase-mediated dUTP-biotin nick end labeling (TUNEL) staining (72 hr) and cleaved caspase 3 staining (48 hr) after doxycycline withdrawal, indicating that apoptosis had been triggered (Figure 3A, bottom row, and Figure S2, respectively). Furthermore, PCNA staining at 48 hr of doxycycline withdrawal showed decreased proliferation of cancer cells (Figure S2).

Consistent with the increased apoptosis and decreased proliferation suggested by TUNEL and PCNA staining, MRI results demonstrated that *EGFR TL*-driven lung tumors completely regressed by 10 days after doxycycline withdrawal (Figure 3B). Microscopic analysis of the lungs from the same mouse that was examined by MRI showed grossly normal lung histology (Figure 3B). No tumor lesions were found in either alveoli or airways after 12 weeks of doxycycline withdrawal in other tumor-bearing mice (data not shown).

To better quantify mutant EGFR expression in tumors at the protein level, we performed western blotting using whole-lung lysates from bitransgenic mice after different durations of doxycycline administration. Although individual differences existed, EGFR phosphorylation was tightly regulated by doxycycline and was synchronized with the presence of tumors (Figure 3C), confirming the essential role of mutant EGFR signaling in tumor maintenance as observed in IHC staining and MRI. Therefore, EGFR remains an attractive therapeutic target for tumors induced in this mouse model.

The Two Types of *EGFR TL* Mutant-Driven Lung Adenocarcinomas Are Resistant to Erlotinib but Show Differing Sensitivities to HKI-272

To investigate the sensitivity of the *EGFR TL*-driven lung tumors to different EGFR-targeted therapies, we serially imaged the bitransgenic mice exposed to continuous doxycycline before and after treatment with erlotinib or HKI-272. After 8–10 weeks of doxycycline treatment, bitransgenic *Tet-op-EGFR TL/CCSP-rtTA* mice were screened by MRI to document the baseline tumor burden. Tumor-bearing mice were then treated orally with erlotinib (four mice), HKI-272 (eight mice), or placebo (three mice) while being kept on continuous doxycycline administration. Erlotinib and HKI-272 were given orally for 2 and 3

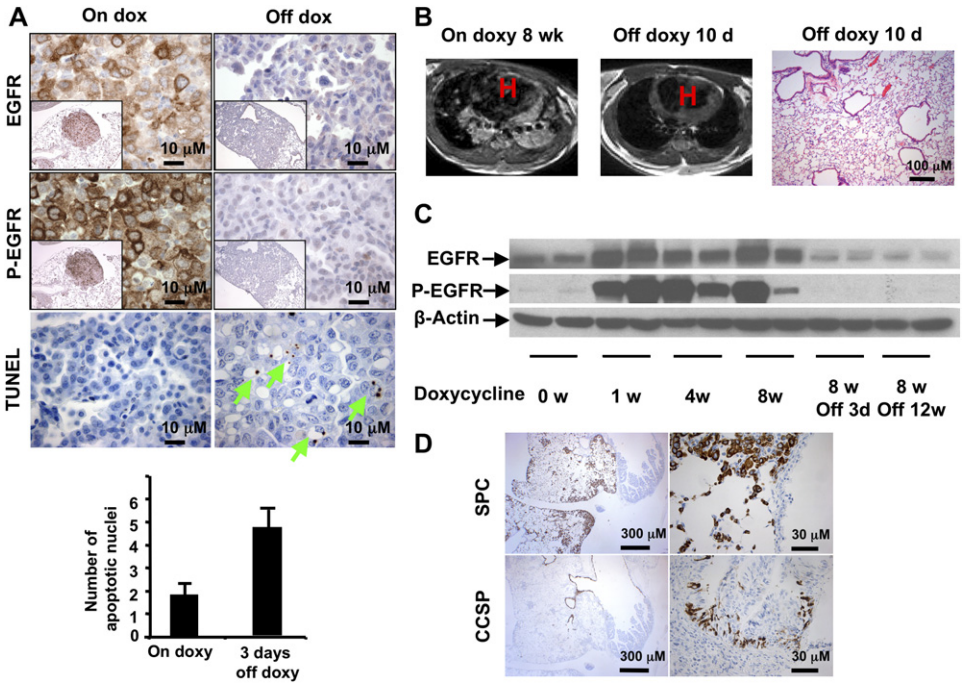

Figure 3. Both Peripheral and Bronchial Tumors Are Dependent on *EGFR TL* Expression for Their Survival but Originate from Different Respiratory Epithelial Cell Types

(A) Peripheral tumors driven by *EGFR T790M-L858R* contained abundant total EGFR protein that was functionally active. Peripheral tumors from *EGFR TL* mice were intensively stained by antibodies against total and phospho-EGFR (Y1068) (top left and middle left panels, respectively). Doxycycline withdrawal completely eliminated the staining by both antibodies in tumors (top right and middle right panels) and also induced apoptosis of tumor cells as indicated by TUNEL staining (bottom row; on doxy, doxycycline administration for 9 weeks; off doxy, doxycycline withdrawal for 3 days after 10 weeks of doxycycline administration; arrow, apoptotic nuclei). Inset in each 800× high-magnification immunohistochemistry photograph shows a low-magnification (80×) photo from the same tumor. Bar diagrams expressed as mean ± SD illustrate the apoptotic indices in lung tumors before and after 3 days of doxycycline withdrawal, determined from at least 200 high-power fields (HPF). Statistical analyses were performed using Student's t test.

(B) Doxycycline withdrawal for 10 days induced complete tumor regression in *EGFR TL* mice. Photographs show MRI scans from a mouse that received 8 weeks of doxycycline diet, before and after doxycycline withdrawal for 10 days (left and middle panels, respectively; H, heart area). H&E staining of the same mouse showed no tumor in either alveoli or bronchioles (right panel).

(C) EGFR and phospho-EGFR expression is synchronized with doxycycline administration. Whole-lung lysates from mice at the indicated time points after doxycycline administration were subjected to western blotting with anti-total EGFR and anti-phospho-EGFR (Y1068) antibodies (top and middle panels, respectively). The analysis for β-actin demonstrates equal loading in each lane (bottom panel).

(D) *EGFR TL*-induced peripheral tumors originated from typed II pneumocytes, while bronchial tumors originated from Clara cells. Sections were stained with antibodies against type II pneumocyte-specific SPC and Clara-cell-specific CCSP (top and bottom rows, respectively).

weeks, respectively, at a daily dose (50 mg/kg) that has been proven to be effective in treating mouse lung adenocarcinomas driven by *EGFR L858R* single mutation (Ji et al., 2006a). None of the *EGFR TL/CCSP-rtTA* mice receiving erlotinib showed significant tumor reduction by MRI. However, in the 8 mice treated with HKI-272, there was a mixed response: some tumor lesions partially regressed, while others grew. Overall, the response favored regression (total regression rate 19.7% ± 3.2% for all eight mice; Figure 4A, left two columns, and Figure 4B). Increasing doses of HKI-272 were then administered to tumor-bearing mice after 8 weeks of doxycycline administration in an experiment in which ten mice were randomized to receive 100 mg/kg or 150 mg/kg daily for 3 weeks. Although HKI-272 was well tolerated at all dosages, the higher doses did not increase the tumor response rate (data not shown).

Histologic analysis of the lungs from mice treated with HKI-272 alone revealed that there was a decreased number of peripheral adenocarcinomas, and significant treatment effect in this lung compartment as demonstrated by decreased cellularity, increased fibrosis, and the presence of necrosis within the residual tumor masses (Figure 4A, bottom row, and data not shown). No significant treatment effect was observed in erlotinib-treated mice or placebo-treated control mice (Figure 4A, middle and top row). In contrast to peripheral tumors, bronchial tumors driven by *EGFR TL* did not respond to either erlotinib or HKI-272 treatment (Figure 4A, far right column). Focal pneumonia with an increased number of intra-alveolar macrophages filling the alveolar spaces was often observed in all the mice, potentially due to airway obstruction by bronchial tumors (Figure 2B, bottom row, second panel from left and far right panel).

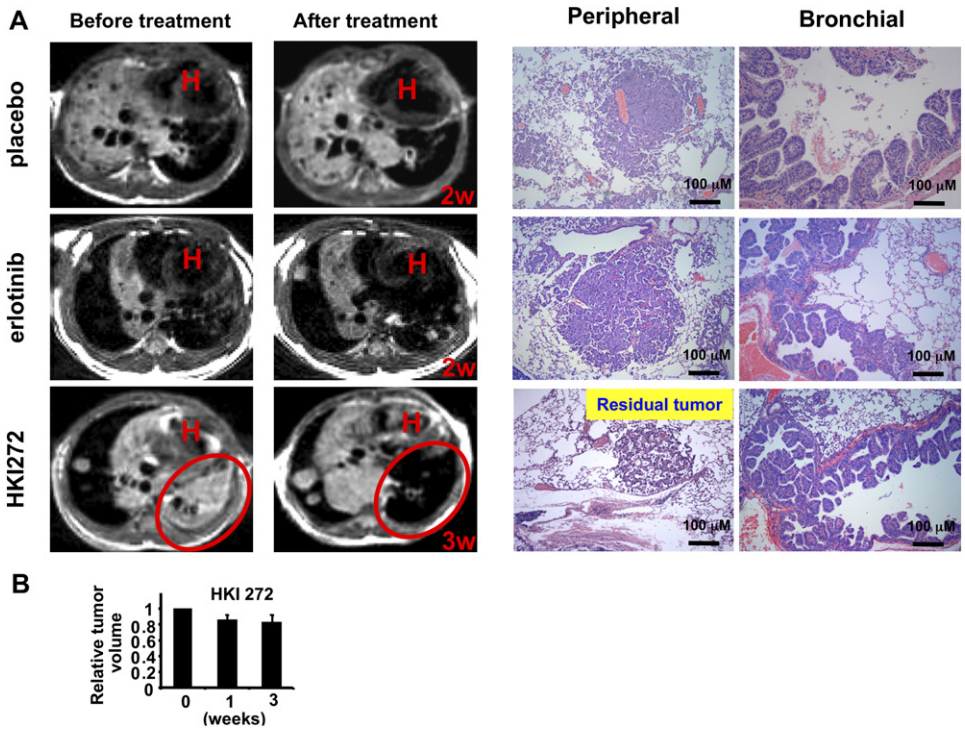

Figure 4. HKI-272, but Not Erlotinib, Is Effective against *EGFR TL*-Driven Peripheral Tumors

(A) HKI-272 generated a mixed radiographic response in *EGFR TL* mice and induced histological treatment effects in peripheral tumors but not bronchial tumors. After approximately 8 to 10 weeks of doxycycline administration, tumor-bearing mice were identified by MRI and divided into different treatment groups (placebo, top row; erlotinib, middle row; HKI-272, bottom row). While doxycycline was continued, all drugs were administered orally at a dose of 50 mg/kg/day for 2 or 3 weeks; the length of drug treatment for individual mice depended on their overall condition. Mice were sacrificed at the indicated times after reimaging. MR images taken before and after drug treatment are shown in the two left columns. Note the increased tumor burden after erlotinib treatment and the mixed response after HKI-272 treatment (H, heart area). Representative H&E staining for both peripheral and bronchial tumors from the lungs of the corresponding mice are shown in the two right columns.

(B) Data (expressed as mean ± SD) illustrate the degree of tumor regression evaluated by MRI. Statistical analysis was performed using Student's two-tailed t test.

Bronchial Tumors Driven by *EGFR TL* Are Sensitive to Combination Therapy with HKI-272 and Rapamycin

Since *EGFR TL*-driven bronchial tumors did not demonstrate a histologic treatment effect after treatment with HKI-272 alone, we tested whether combination therapy with rapamycin could produce response. Rapamycin is a specific inhibitor of mTOR, an important downstream component of the EGFR/PI3K/Akt signaling pathway. Five tumor-bearing mice were treated daily with HKI-272 (50 mg/kg, oral gavage) and rapamycin (2 mg/kg, i.p. injection) combination therapy for 3 weeks. Control mice were treated with erlotinib and rapamycin combination therapy or rapamycin alone (four mice in each group) with a similar dosing schedule. A significant reduction in tumor volume (72% ± 4.5%) was observed in the HKI-272 plus rapamycin treatment group by MRI after a 3 week period, but no significant tumor regression was found in either erlotinib plus rapamycin or rapamycin alone groups (Figure 5A, left two columns, and Figure 5B). Pathological examination of mice from the respective treatment groups confirmed the MRI findings. Residual tumors from mice in the HKI-272 and rapamycin combination treatment group demonstrated significant treatment effects in both peripheral and bronchial tumors, with fewer tumors, decreased cellularity, and increased fibrosis and necrosis. Tumors from control treatment groups remained unaffected (Figure 5A, right two columns, and data not shown).

HKI-272 and Rapamycin Synergistically Suppress the PI3K-mTOR Axis Driven by EGFR TL Both In Vitro and In Vivo

H1975 cells express EGFR harboring the TL compound mutation and are resistant to erlotinib. Although HKI-272 was reported to suppress the growth of these cells (Kwak et al., 2005; Shimamura et al., 2006), the IC_{50} was approximately 47 times higher than that for the H3255 cell line expressing an EGFR L858R mutation (222.45 nM versus 4.78 nM; Figure 6A). The hypersensitivity of H3255 cells to HKI-272 is consistent with previous results evaluating its efficacy in murine model of lung cancer promoted by *EGFR L858R*. Therefore, these in vitro results suggest that the presence of the T790M resistance mutation greatly hinders the efficacy of HKI-272.

The significant response of *EGFR TL* mice to HKI-272 and rapamycin combination treatment led us to evaluate

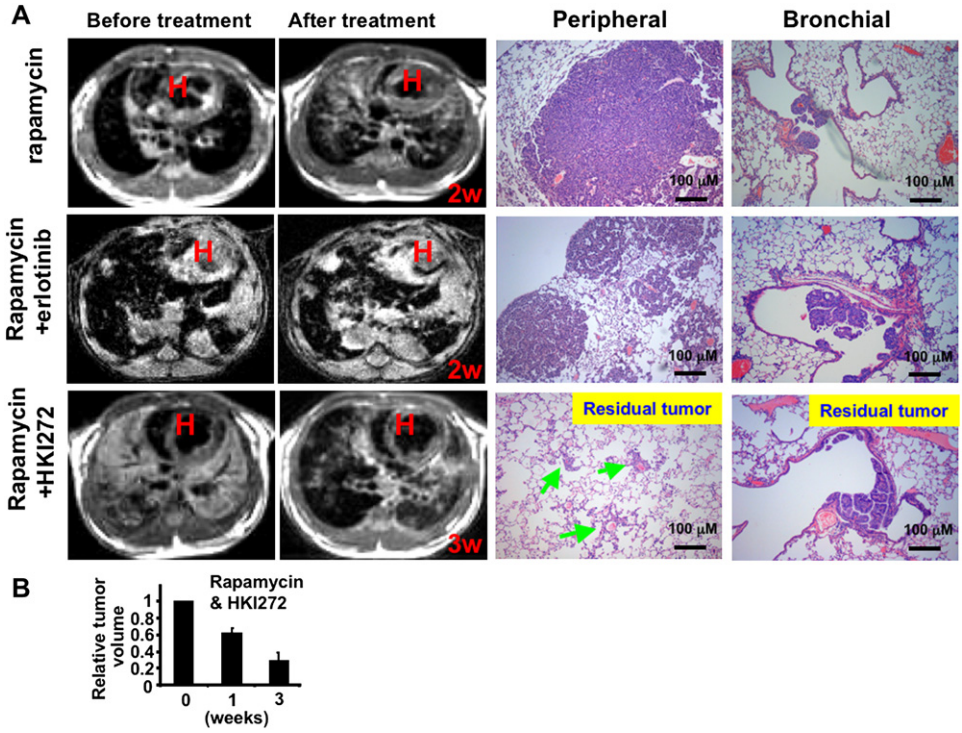

Figure 5. Combination Therapy of HKI-272 and Rapamycin Is Effective for Both Peripheral and Bronchial Tumors, While the Combination of Erlotinib and Rapamycin Has No Effects

(A) HKI-272 combined with rapamycin caused dramatic tumor regression by MRI and induced significant histological treatment effects in both bronchial and peripheral tumors. Treatment groups and panel designations are similar to those of Figure 4A, except that all mice also received a daily i.p. injection of 2 mg/kg rapamycin (arrows indicate residual tumors; H, heart area).

(B) Data (expressed as mean ± SD) illustrate the degree of tumor regression evaluated by MRI. Statistical analysis was performed using Student's two-tailed t test.

the potential synergism between these two drugs. As shown in Figure 6B, we treated a panel of NSCLC cell lines with different *EGFR* mutational status [H1975 (TL), H3255 (L858R), H820 (E746_T751del-T790M), and HCC827 (E746_A750 del)] with varying concentrations of HKI-272 or rapamycin alone or in combination at a 1:50 ratio. None of the NSCLC cell lines tested were sensitive to treatment with rapamycin alone. H3255 cells and HCC827 cells, which harbor L858R and deletion EGFR kinase domain mutations, respectively, were exquisitely sensitive to HKI-272 alone, and the sensitivity of these cells was not significantly improved by addition of rapamycin. In contrast, for NSCLC cell lines harboring T790M secondary mutations, combination treatment was synergistic, indicated by a marked reduction in cell survival. For example, in H1975 cells, a 2.5-fold decrease in the IC_{50} value of HKI-272 (244 nM versus 92 nM) was observed in the presence of rapamycin (combination index [CI] = 0.762). Strikingly, these drugs showed even stronger synergy in H820 cells, as the IC_{50} of HKI-272 was reduced from more than 10 μM to 101 nM in the presence of rapamycin (CI = 0.664).

To elucidate the mechanisms of HKI-272-rapamycin synergy in cells harboring an EGFR T790M secondary mutation, the intracellular signaling responses of H1975 cells and H3255 cells treated with HKI-272 or rapamycin alone or in combination were compared (Figure 6C). In HKI-272-sensitive H3255 cells, HKI-272 alone was sufficient to completely dephosphorylate ErbB family kinases including EGFR (Tyr^{1068}), ErbB2 ($Tyr^{1221/1222}$), and ErbB3 (Tyr^{1289}). The receptor tyrosine kinase (RTK) inactivation resulted in reduced phosphorylation of Akt (Ser^{473}), with downstream inhibition of mTOR, as evidenced by reduced phosphorylation of p70S6K (Thr^{389}) and S6 ($Ser^{240/244}$). Reduced phosphorylation of Akt, p70S6K, and S6K persisted for 24 hr and was evident on long exposure of the respective blots. As expected, rapamycin reduced phosphorylation of p70S6K (Thr^{389}) and S6 ($Ser^{240/244}$) downstream of mTOR, accompanied by increased phosphorylation of Akt, consistent with previous reports suggesting that rapamycin treatment suppresses a negative feedback loop, resulting in activation of PI3K (Easton et al., 2006; O'Reilly et al., 2006). The treatment of H3255 cells with HKI-272 and rapamycin in combination caused a marked reduction in phosphorylation of Akt, p70S6K, and S6 that was similar to that observed with HKI-272 alone (Figure 6C and Table S1).

In contrast to H3255 cells, H1975 cells treated with HKI-272 resulted in reduced phosphorylation of EGFR (Tyr^{1068}), ErbB2 ($Tyr^{1221/1222}$), and ErbB3 (Tyr^{1289}), but residual phosphorylation of EGFR was detectable, as shown

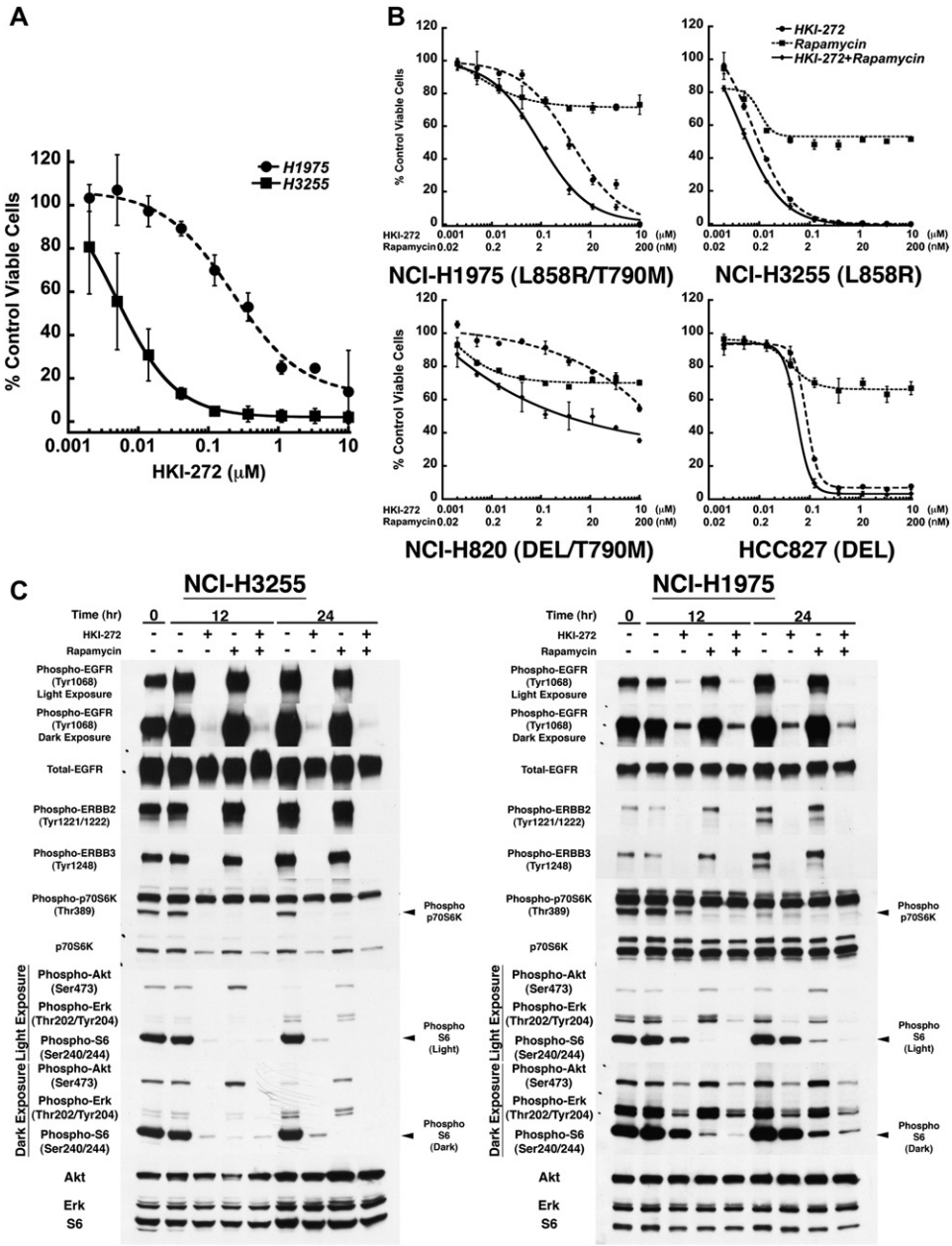

Figure 6. HKI-272 and Rapamycin Synergistically Suppress the PI3K-mTOR-S6k-S6 Axis, which Is Critical for Survival and Proliferation of NSCLC Cells

(A) The IC_{50} of HKI-272 was far lower in H3255 (*EGFR L858R*) cells than that of H1975 (*EGFR TL*) cells. H3255 cells and H1975 cells were treated with HKI-272 at the indicated concentrations in cell proliferation assays as described in the Experimental Procedures. The survival of each sample was normalized compared to that of control DMSO-treated cells. The data points shown represent the average of normalized values ± standard error from two independent experiments.

(B) HKI-272 and rapamycin were synergistic in NSCLC cells harboring T790M *EGFR* secondary mutations. H1975, H3255, H820, and HCC827 cells were treated with the indicated concentrations of HKI-272 alone, rapamycin alone, or the two drugs concomitantly in cell proliferation assays. The survival of each sample was normalized to that of control DMSO-treated cells. The data points shown represent the average of normalized values ± standard error from three independent experiments. Combination indices (CI) were calculated as described in the Experimental Procedures, demonstrating synergy in H1975 and H820 cells.

(C) HKI-272 incompletely suppresses the EGFR-Akt-mTOR-S6 axis in H1975 cells. Exponentially growing H1975 or H3255 cells were treated with vehicle (DMSO), HKI-272 (800 nM), rapamycin (16 nM), or combined HKI-272 (800 nM) and rapamycin (16 nM). At the indicated time points, whole-cell lysates were harvested and subjected to SDS-PAGE, followed by western blotting with the indicated antibodies. Phosphorylation of Akt, Erk, S6K, and S6 was effectively reduced by HKI-272 alone in H3255 cells. However, a similar degree of dephosphorylation of these proteins required the combination of HKI-272 and rapamycin in H1975 cells.

on long exposure of the phospho-EGFR (Tyr^{1068}) blot (Figure 6C). HKI-272 treatment did not lead to complete inactivation of secondary signaling molecules, including Akt and Erk, as evidenced by the residual phosphorylation persisting on Akt (Ser^{473}) and Erk (Thr^{202}/Tyr^{204}), demonstrated on long exposure of the respective blots. Similarly, mTOR signaling was incompletely abrogated by HKI-272 treatment, as p70S6K (Thr^{389}) and S6 ($Ser^{240/244}$) remained phosphorylated (Table S1). In contrast to the complete dephosphorylation of S6 in H3255 cells by HKI-272 treatment, the reduction in S6 phosphorylation at $Ser^{240/244}$ in H1975 cells was modest and reversed within 24 hr. As in H3255 cells, rapamycin treatment of H1975 cells resulted in reduced phosphorylation of S6 by 12 hr, with increased Akt phosphorylation over time.

Most importantly, HKI-272 and rapamycin combination treatment of H1975 cells inhibited not only EGFR phosphorylation but also downstream PI3K-Akt and mTOR signaling. Identical results were obtained using H820 (E746_T751del-T790M) cells treated with HKI-272, rapamycin, or the HKI-272-rapamycin combination (data not shown). These data are consistent with the synergy of HKI-272 and rapamycin in cell lines with the T790M secondary mutation and support the superior treatment effects of combination therapy observed in the EGFR TL animal model.

To confirm the in vitro data, mice bearing *EGFR TL*-driven tumors were treated with HKI-272, rapamycin, and the combination of both drugs for 48 hr, followed by immunohistochemical staining of signaling molecules including phospho-EGFR, phospho-ErbB2, phospho-ErbB3, phospho-Akt, phospho-MAPK, and phospho-S6. HKI-272 alone effectively decreased the expression level of phospho-EGFR and ErbB2, but not ErbB3 in peripheral tumors. While downstream signaling of ErbB family members such as Akt and MAPK were also inhibited, expression of phospho-S6 was not altered dramatically with HKI-272 monotherapy. Rapamycin alone significantly decreased phospho-S6 staining in peripheral tumors, while phospho-EGFR, ErbB2, ErbB3, Akt, and phospho-MAPK remained intact. In contrast, the combination of the two drugs strongly inhibited phospho-EGFR, ErbB2, and phospho-S6 staining as well as phospho-Akt and MAPK in peripheral tumors and induced a dramatic increase in caspase 3 staining (Figure 7 and Figure S3). Bronchial tumors demonstrated a response pattern similar to that observed in peripheral tumors, although to a lesser degree (data not shown), potentially due to higher baseline levels of expression of EGFR, ErbB2, and ErbB3 (Figure S1), as well as Akt and S6 (data not shown). In summary, these data demonstrate that HKI-272 and rapamycin combination therapy inhibits both upstream and downstream signaling of the EGFR/PI3K/mTOR axis both in vitro and in vivo, accounting for the cytotoxic synergy of these drugs.

DISCUSSION

In the current study, we demonstrate that *EGFR* harboring the compound kinase domain L858R and T790M mutation is oncogenic in vivo. As expected, these tumors are resistant to erlotinib despite retaining full addiction to EGFR signaling for survival, thereby validating that the mutant EGFR remains a promising therapeutic target, even in the setting of erlotinib resistance.

We were initially surprised that *EGFR TL*-driven tumors demonstrated a suboptimal response to the irreversible TKI HKI-272. HKI-272 was initially reported to be sufficient to inhibit growth of the H1975 lung cancer cell line with the *EGFR TL* mutation (Kwak et al., 2005) that is resistant to erlotinib. However, our data indicate that the efficacy of the drug appears to be greater against cells expressing *EGFR* harboring the L858R point mutation alone. These results are also supported by the relative potency of HKI-272 in a Ba/F3 system with artificial expression of either *EGFR TL* or *EGFR L858R* (Ji et al., 2006b). Consistent with these in vitro data, HKI-272 demonstrated excellent activity against lung adenocarcinomas driven by *EGFR L858R* (Ji et al., 2006a), but limited efficacy against peripheral tumors driven by *EGFR TL*, and no efficacy against EGFR TL-driven bronchial tumors. Importantly, this result is concordant with emerging preliminary data from a multisite phase I clinical trial of HKI-272. In this initial experience, although 5 of 12 previously treated NSCLC patients achieved stable disease of varying duration up to 24 weeks, no confirmed partial responses were observed (K.K. Wong et al., 2006, J. Clin. Oncol., abstract). Thus, the therapeutic studies in our mouse model may be reflective of the clinical activity observed in ongoing human lung cancer HKI-272 trials.

The PI3K-mTOR axis is a pivotal pathway downstream of EGFR that governs the sensitivity of NSCLC cells to EGFR TKIs (Engelman and Cantley, 2006; Engelman et al., 2005). This view is supported by the finding that erlotinib synergizes with rapamycin in a subset of NSCLC harboring wild-type *EGFR* (Buck et al., 2006). Experiments in *EGFR TL*-driven cell lines revealed that rapamycin synergizes with HKI-272 to inhibit survival. Unlike HKI-272 alone, the combination abrogates the PI3K/Akt and mTOR pathway more effectively. These results are also reflected in vivo, where HKI-272 and rapamycin combination therapy induces much more dramatic tumor regression than HKI-272 monotherapy in our *EGFR TL*-driven mouse model. Taken together, the data suggest that the treatment strategy of irreversible EGFR inhibition and mTOR inhibition may induce a more promising response rate against NSCLC with acquired erlotinib resistance.

Our work points to a potential limitation of irreversible inhibitors against EGFR harboring a T790M secondary kinase domain mutation, since mTOR signaling may not be completely suppressed. The results in H1975 cells suggest that even minimal EGFR activity may be sufficient to maintain significant mTOR activity, so that the potency of EGFR TL inhibition by an irreversible inhibitor is a critical issue. Our data do not rule out the possibility that other irreversible EGFR/ErbB2 inhibitors will have improved potency to cause more complete suppression of the EGFR-Akt-mTOR-S6 axis and therefore will not require rapamycin-mediated synergism to achieve response in

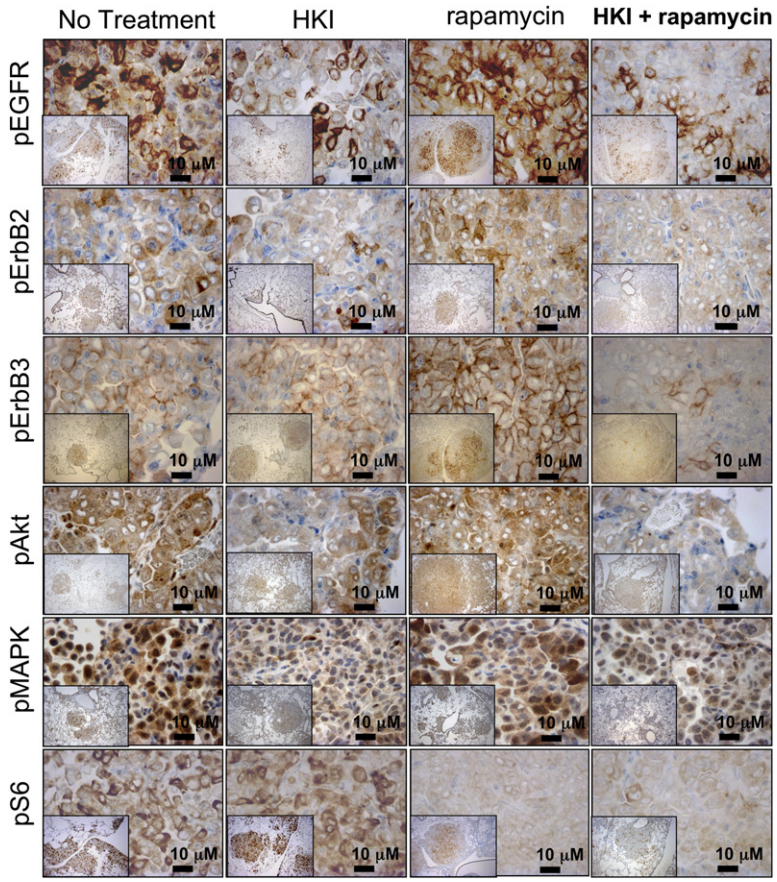

Figure 7. Immunohistochemical Assessment Reveals that Phosphorylation of EGFR Family Members and Downstream Signaling Molecules Respond Differently to HKI-272, Rapamycin, or the Combination of Both Drugs

EGFR TL mice were treated with HKI-272, rapamycin, or the combination therapy for 48 hr, and lung sections were then stained with antibodies recognizing phospho-EGFR, phospho-ErbB2, phospho-ErbB3, phospho-Akt, phospho-MAPK, and phospho-S6. Photos shown are representative fields from duplicate animals in each group. IHC photographs show low-magnification (100×) pictures (insets) and high-magnification (800×) pictures.

tumors harboring a T790M mutation. Lastly, our data do not exclude the possibility that, in lung cancer cells harboring *EGFR TL*, engagement of alternative signaling pathways downstream of other receptor tyrosine kinases may independently activate the mTOR axis when EGFR is inhibited.

Despite the importance of mTOR signaling, lung adenocarcinomas driven by *EGFR TL* are relatively insensitive to growth inhibition by rapamycin alone. Although phospho-S6 may be important for the tumor maintenance in these *EGFR TL*-driven lung cancers, its inhibition is not sufficient to halt tumor growth. In addition, we observed enhanced phosphorylation of Akt in response to rapamycin. This increase in Akt phosphorylation is consistent with the finding that the rapamycin analog RAD001 results in increased Akt phosphorylation in human lung tumors (O'Reilly et al., 2006). However, because PI3K is primarily driven by EGFR-mediated phosphorylation of ErbB3 in these cancers (Engelman et al., 2005), rapamycin is unlikely to have the untoward side effect of increasing Akt signaling when combined with HKI-272 in this setting (consistent with the observations in Figure 6). We have also confirmed that erlotinib was unable to synergize with rapamycin to compromise the survival of the NSCLC harboring EGFR T790M secondary mutation, again indicating the need to effectively inhibit EGFR and other upstream signaling events.

Although HKI-272 alone had limited efficacy against peripheral tumors, bronchial tumors were completely resistant. The mechanistic basis for the relative resistance of the bronchial tumors to HKI-272 remains unclear, but it is possible that there may be differences in the ratio and composition of EGFR homodimers and heterodimers in bronchial and alveolar epithelial cells. Interestingly, HKI-272 is expected to bind to an inactive conformation of the EGFR, in which the so-called C helix is displaced from the active site. Activating dimerization interactions have been shown to push the C helix into its active conformation (Zhang et al., 2006) and would therefore be expected to prevent efficient binding of HKI-272. Thus, potential differences in ligand expression in these two tumor environments could explain the relative lack of sensitivity to HKI-272 in the bronchial tumors. We have indeed observed that the intensity of phospho-EGFR, ErbB2, and ErbB3 staining is higher in bronchial than peripheral tumors (Figure S1), supporting this hypothesis.

The EGFR TL double mutation may also alter the extent of heterodimerization with ErbB3, or the efficiency of phosphorylation of the ErbB3 sites that recruit and activate PI3K, which could lead to tumors in bronchial epithelium where this ErbB family member or its ligand are more highly expressed. Of note, normal bronchial epithelium is positive for phosphorylated EGFR and ErbB2 staining, while positive IHC staining of these proteins is almost

absent in alveolar epithelium (Figure 3A and Figure S1). Additionally, we have observed that activated mutant ErbB2 induces tumors in the lung bronchial epithelium (unpublished data). Therefore, the existence of *EGFR TL*-driven tumors in ErbB2-expressing bronchial epithelia suggests that EGFR /ErbB2 heterodimers may play an important role in both *EGFR*- and *ErbB2*-initiated mouse lung cancers, thereby supporting the hypothesis that ErbB2 and EGFR signaling work synergistically in at least a subset of *EGFR*-driven lung tumors (Cappuzzo et al., 2005). Since bronchial tumors are absent in the either *EGFR L858R*- or *EGFR T790M*-driven mouse lung cancer model (Ji et al., 2006a and unpublished data), it is possible that an unique EGFR/ErbB2 interaction only exists between ErbB2 and EGFR TL but not the EGFR single point mutation (L858R or T790M). It is also possible that, in the EGFR TL mice, the expression levels of ErbB2 and ErbB3 might be different in the alveolar and bronchial compartments and thus contribute to the observed phenotype.

Although an EGFR/ErbB2 dual inhibitor like HKI-272 should theoretically inhibit function of both EGFR/ErbB3 and ErbB2/ErbB3 heterodimers, our IHC data show that HKI-272 did not completely block phospho-ErbB2 and EGFR signaling, even when the HKI-272 dose was increased to 150 mg/kg/day (data not shown). Achievable concentrations of the drug in different types of tumors may also be different due to different diffusion barriers in bronchial and peripheral tumors. Recently, Sergina et al. showed that residual ErbB2 kinase activity can drive refractory ErbB3 phosphorylation in multiple cell lines and xenograft animal models (Sergina et al., 2007), which may partially explain our observations in the de novo transgenic lung cancer model.

Bronchiolar Clara cells and alveolar type II pneumocytes arise from the same precursor cells (Kim et al., 2005). Existence of both bronchial and peripheral tumors in our *EGFR TL*-driven lung cancer mouse model, as well as distinct SPC and CCSP staining patterns of these two types of tumors, suggest that the oncogene was actually expressed in the precursor cells that possess the potential to differentiate into both Clara cells and type II pneumocytes. However, it remains unclear why the *EGFR TL* double mutation gives rise to bronchial tumors, while the L858R single mutation does not. It is likely that the double mutation "hyperactivates" the kinase. The equivalent of the T790M residue is well known from the earliest studies of other oncogenic tyrosine kinases and has been termed the "gatekeeper" residue because the presence of large versus small amino acids in this position controls access to a pocket that can be exploited in inhibitor design. The corresponding mutation introduced into c-Src confers a transforming phenotype (Kato et al., 1986). The equivalent mutation also arises in Bcr-Abl (T315I) in imatinib-treated CML patients, where it confers inhibitor resistance, and has also been shown to pre-exist in nontreated populations (Bell et al., 2005). These findings indicate that the mutation may be an activating mutation in these kinases, or may otherwise confer a selective advantage even in the absence of inhibitor. Thus, the T790M mutation may lead to a higher degree of catalytic activation of the EGFR, particularly in concert with other activating mutations, such as L858R. This hypothesis is particularly attractive given the discovery that a single *EGFR TL* allele confers gefitinib resistance in a lung cancer cell line with more than 40 amplified EGFR alleles (Engelman et al., 2006).

In summary, we have generated a mouse model of lung adenocarcinoma driven by *EGFR TL* that mimics human lung cancers with acquired resistance to erlotinib. We observed that combination therapy involving the irreversible EGFR/ErbB2 TKI HKI-272 and the mTOR inhibitor rapamycin led to dramatic tumor regression. Our study suggests that an irreversible TKI combined with rapamycin or other rapamycin analogs such as CCI-779 or RA0001 may be of benefit to NSCLC patients with T790M-mediated acquired erlotinib resistance. This animal model may be of value in screening newer-generation EGFR inhibitors as well as other therapeutic agents and drug combinations prior to human clinical trials and provides a platform to study crosstalk between different oncogenic or tumor suppressor signaling pathways and aberrant EGFR signaling.

EXPERIMENTAL PROCEDURES

Generation of the *CCSP-rtTA/Tet-op-EGFR TL* Mouse Cohort

To generate the *Tet-op-EGFR TL* transgenic mice, site-directed mutagenesis was performed on the pCIBA-*hEGFR* plasmid (provided by Dr. Nabeel Bardeesy). The fragment containing the whole *hEGFR* ORF with the Kozak site was then subcoloned into pTRE2-hyg (Clontech, Mountain View, CA). The constructs were then digested to release the entire allele containing *Tet-op-EGFR TL-β-globin* polyA. Transgenic mice were then generated by injection of the construct into FVB/N blastocysts. Progeny were genotyped and characterized as described in the Supplemental Data. All mice were housed in a pathogen-free environment at the Harvard School of Public Health and were handled in strict accordance with Good Animal Practice as defined by the Office of Laboratory Animal Welfare, and all animal work was done with Dana-Farber Cancer Institute IACUC approval.

RT-PCR and Quantitative PCR

Total RNA samples were prepared as previously described (Ji et al., 2006a) and then retrotranscribed into first-strand cDNA using the Superscript First Strand Synthesis System following the manufacturer's protocol (Invitrogen, Carlsbad, CA). Quantitative PCR was performed by monitoring the increase in fluorescence of SYBR green dye in real-time (Qiagen, Valencia, CA) with an ABI 7700 sequence detection system (PerkinElmer Life Sciences, Waltham, MA). Primers used for RT-PCR and real-time PCR are listed in the Supplemental Data.

Immunohistochemistry and TUNEL Assays

Mice were sacrificed and left lungs were snap frozen; right lungs were fixed in 10% formalin, embedded in paraffin, and sectioned at 5 μm, as described previously (Ji et al., 2006a). Histological analyses were performed as described in the Supplemental Data.

Targeted Therapy Using the EGFR Inhibitors HKI272, Erlotinib, and/or Rapamycin

After continuously exposure to doxycycline diets for more than 8 weeks, bitransgenic mice were subjected to MRI to document the lung tumor burden. After initial imaging, either HKI-272 (Wyeth Pharmaceuticals, Pearl River, NY) or erlotinib (Biaffin GmbH & Co KG, Kassel, Germany) formulated in 0.5% methocellulose-0.4%

polysorbate-80 (Tween 80) were administrated by gavage at 50 mg/kg daily. Rapamycin (LC laboratories, Woburn, MA) formulated in 5% PEG400 and 5% Tween 80 was administrated by i.p. injection at 2 mg/kg daily. The same mice were imaged by MRI to determine the reduction in tumor volume weekly during the respective treatments and then sacrificed for further histological and biochemical studies. HKI-272 treatment was continued for 3 weeks to induce maximal tumor response. Erlotinib treatment was stopped after 2 weeks due to increasing tumor burden. Littermates were used as control for all treatment groups.

Tumor Cell Lines and Drug Treatment

NCI-H1975, NCI-H3255, and NCI-H820 NSCLC cell lines (designated H1975, H3255, and H820, respectively) were obtained from the American Type Culture Collection (Rockville, MD), and HCC827 cells were generously provided by Dr. Adi Gazdar. All cell lines were maintained in the recommended growth medium.

Both HKI-272 and rapamycin were reconstituted in DMSO (10 mM and 100 μM as stock solution) and used at the indicated concentrations.

Cell Proliferation Assays and Western Blot Analysis

MTT assay and western blotting were done as described in the Supplemental Data (Shimamura et al., 2005). Combination indices (CI) were calculated by the Median Effect Method, available on Calcusyn (Biosoft, Cambridge, UK).

MRI Scanning and Tumor Volume Measurement

MRI scanning and tumor volume measurement were described elsewhere and in the Supplemental Data (Li et al., 2007).

Statistics

Statistical analyses were performed using unpaired two-tailed Student's t test. p values of less than 0.05 were considered significant.

Supplemental Data

The Supplemental Data include Supplemental Experimental Procedures, three supplemental figures, and one supplemental table and can be found with this article online at http://www.cancercell.org/cgi/content/full/12/1/81/DC1/.

ACKNOWLEDGMENTS

We thank Dr. William Pao and Dr. Maureen Zakowski for confirmation of histological analyses in our animal model; Dr. Jeffrey Whitsett for providing the *CCSP-rtTA* transgenic mice. We also thank Christine Lam and Mei Zheng for technical supports. This work was supported by the Sidney Kimmel Foundation for Cancer Research (K.-K.W.); the Joan Scarangello Foundation to Conquer Lung Cancer (K.-K.W.); the Flight Attendant Medical Research Institute (K.-K.W.); and NIH grants K08 AG024004 (K.-K.W.), R01 AG2400401 (K.-K.W.), R01 CA122794 (K.-K.W.), P20 CA90578 (G.I.S. and L.R.C.), and R01 CA90687 (G.I.S.). T.S. is supported by a Career Development Award as part of the Dana-Farber/Harvard Cancer Center Specialized Program of Research Excellence (SPORE) in Lung Cancer, and NIH grant P20 CA90578.

Received: February 6, 2007
Revised: April 3, 2007
Accepted: June 5, 2007
Published: July 9, 2007

REFERENCES

Bell, D.W., Gore, I., Okimoto, R.A., Godin-Heymann, N., Sordella, R., Mulloy, R., Sharma, S.V., Brannigan, B.W., Mohapatra, G., Settleman, J., and Haber, D.A. (2005). Inherited susceptibility to lung cancer may be associated with the T790M drug resistance mutation in EGFR. Nat. Genet. *37*, 1315–1316.

Buck, E., Eyzaguirre, A., Brown, E., Petti, F., McCormack, S., Haley, J.D., Iwata, K.K., Gibson, N.W., and Griffin, G. (2006). Rapamycin synergizes with the epidermal growth factor receptor inhibitor erlotinib in non-small-cell lung, pancreatic, colon, and breast tumors. Mol. Cancer Ther. *5*, 2676–2684.

Cappuzzo, F., Hirsch, F.R., Rossi, E., Bartolini, S., Ceresoli, G.L., Bemis, L., Haney, J., Witta, S., Danenberg, K., Domenichini, I., et al. (2005). Epidermal growth factor receptor gene and protein and gefitinib sensitivity in non-small-cell lung cancer. J. Natl. Cancer Inst. *97*, 643–655.

Conde, E., Angulo, B., Tang, M., Morente, M., Torres-Lanzas, J., Lopez-Encuentra, A., Lopez-Rios, F., and Sanchez-Cespedes, M. (2006). Molecular context of the EGFR mutations: Evidence for the activation of mTOR/S6K signaling. Clin. Cancer Res. *12*, 710–717.

Easton, J.B., Kurmasheva, R.T., and Houghton, P.J. (2006). IRS-1: Auditing the effectiveness of mTOR inhibitors. Cancer Cell *9*, 153–155.

Engelman, J.A., Janne, P.A., Mermel, C., Pearlberg, J., Mukohara, T., Fleet, C., Cichowski, K., Johnson, B.E., and Cantley, L.C. (2005). ErbB-3 mediates phosphoinositide 3-kinase activity in gefitinib-sensitive non-small cell lung cancer cell lines. Proc. Natl. Acad. Sci. USA *102*, 3788–3793.

Engelman, J.A., and Cantley, L.C. (2006). The role of the ErbB family members in non-small cell lung cancers sensitive to epidermal growth factor receptor kinase inhibitors. Clin. Cancer Res. *12*, 4372s–4376s.

Engelman, J.A., Mukohara, T., Zejnullahu, K., Lifshits, E., Borras, A.M., Gale, C.M., Naumov, G.N., Yeap, B.Y., Jarrell, E., Sun, J., et al. (2006). Allelic dilution obscures detection of a biologically significant resistance mutation in EGFR-amplified lung cancer. J. Clin. Invest. *116*, 2695–2706.

Fisher, G.H., Wellen, S.L., Klimstra, D., Lenczowski, J.M., Tichelaar, J.W., Lizak, M.J., Whitsett, J.A., Koretsky, A., and Varmus, H.E. (2001). Induction and apoptotic regression of lung adenocarcinomas by regulation of a K-Ras transgene in the presence and absence of tumor suppressor genes. Genes Dev. *15*, 3249–3262.

Hay, N. (2005). The Akt-mTOR tango and its relevance to cancer. Cancer Cell *8*, 179–183.

Hay, N., and Sonenberg, N. (2004). Upstream and downstream of mTOR. Genes Dev. *18*, 1926–1945.

Ji, H., Li, D., Chen, L., Shimamura, T., Kobayashi, S., McNamara, K., Mahmood, U., Mitchell, A., Sun, Y., Al-Hashem, R., et al. (2006a). The impact of human EGFR kinase domain mutations on lung tumorigenesis and in vivo sensitivity to EGFR-targeted therapies. Cancer Cell *9*, 485–495.

Ji, H., Zhao, X., Yuza, Y., Shimamura, T., Li, D., Protopopov, A., Jung, B.L., McNamara, K., Xia, H., Glatt, K.A., et al. (2006b). Epidermal growth factor receptor variant III mutations in lung tumorigenesis and sensitivity to tyrosine kinase inhibitors. Proc. Natl. Acad. Sci. USA *103*, 7817–7822.

Johnson, B.E., Jackman, D., and Janne, P.A. (2006). Impact of EGFR mutations on treatment of non-small cell lung cancer. Cancer Chemother. Pharmacol. *58* (*Suppl 7*), 5–9.

Kato, J.Y., Takeya, T., Grandori, C., Iba, H., Levy, J.B., and Hanafusa, H. (1986). Amino acid substitutions sufficient to convert the nontransforming p60c-src protein to a transforming protein. Mol. Cell. Biol. *6*, 4155–4160.

Kim, C.F., Jackson, E.L., Woolfenden, A.E., Lawrence, S., Babar, I., Vogel, S., Crowley, D., Bronson, R.T., and Jacks, T. (2005). Identification of bronchioalveolar stem cells in normal lung and lung cancer. Cell *121*, 823–835.

Kobayashi, S., Boggon, T.J., Dayaram, T., Janne, P.A., Kocher, O., Meyerson, M., Johnson, B.E., Eck, M.J., Tenen, D.G., and Halmos,

B. (2005a). EGFR mutation and resistance of non-small-cell lung cancer to gefitinib. N. Engl. J. Med. *352*, 786–792.

Kobayashi, S., Ji, H., Yuza, Y., Meyerson, M., Wong, K.K., Tenen, D.G., and Halmos, B. (2005b). An alternative inhibitor overcomes resistance caused by a mutation of the epidermal growth factor receptor. Cancer Res. *65*, 7096–7101.

Kwak, E.L., Sordella, R., Bell, D.W., Godin-Heymann, N., Okimoto, R.A., Brannigan, B.W., Harris, P.L., Driscoll, D.R., Fidias, P., Lynch, T.J., et al. (2005). Irreversible inhibitors of the EGF receptor may circumvent acquired resistance to gefitinib. Proc. Natl. Acad. Sci. USA *102*, 7665–7670.

Li, D., Ji, H., Zaghlul, S., McNamara, K., Liang, M.C., Shimamura, T., Kubo, S., Takahashi, M., Chirieac, L.R., Padera, R.F., et al. (2007). Therapeutic anti-EGFR antibody 806 generates responses in murine de novo EGFR mutant-dependent lung carcinomas. J. Clin. Invest. *117*, 346–352.

Manning, B.D. (2004). Balancing Akt with S6K: Implications for both metabolic diseases and tumorigenesis. J. Cell Biol. *167*, 399–403.

O'Reilly, K.E., Rojo, F., She, Q.B., Solit, D., Mills, G.B., Smith, D., Lane, H., Hofmann, F., Hicklin, D.J., Ludwig, D.L., et al. (2006). mTOR inhibition induces upstream receptor tyrosine kinase signaling and activates Akt. Cancer Res. *66*, 1500–1508.

Pao, W., Miller, V.A., Politi, K.A., Riely, G.J., Somwar, R., Zakowski, M.F., Kris, M.G., and Varmus, H. (2005). Acquired resistance of lung adenocarcinomas to gefitinib or erlotinib is associated with a second mutation in the EGFR kinase domain. PLoS Med *2*, e73. 10.1371/journal.pmed.0020073.

Politi, K., Zakowski, M.F., Fan, P.D., Schonfeld, E.A., Pao, W., and Varmus, H.E. (2006). Lung adenocarcinomas induced in mice by mutant EGF receptors found in human lung cancers respond to a tyrosine kinase inhibitor or to down-regulation of the receptors. Genes Dev. *20*, 1496–1510.

Riely, G.J., Politi, K.A., Miller, V.A., and Pao, W. (2006). Update on epidermal growth factor receptor mutations in non-small cell lung cancer. Clin. Cancer Res. *12*, 7232–7241.

Sergina, N.V., Rausch, M., Wang, D., Blair, J., Hann, B., Shokat, K.M., and Moasser, M.M. (2007). Escape from HER-family tyrosine kinase inhibitor therapy by the kinase-inactive HER3. Nature *445*, 437–441.

Shepherd, F.A., Rodrigues Pereira, J., Ciuleanu, T., Tan, E.H., Hirsh, V., Thongprasert, S., Campos, D., Maoleekoonpiroj, S., Smylie, M., Martins, R., et al. (2005). Erlotinib in previously treated non-small-cell lung cancer. N. Engl. J. Med. *353*, 123–132.

Shigematsu, H., and Gazdar, A.F. (2006). Somatic mutations of epidermal growth factor receptor signaling pathway in lung cancers. Int. J. Cancer *118*, 257–262.

Shimamura, T., Lowell, A.M., Engelman, J.A., and Shapiro, G.I. (2005). Epidermal growth factor receptors harboring kinase domain mutations associate with the heat shock protein 90 chaperone and are destabilized following exposure to geldanamycins. Cancer Res. *65*, 6401–6408.

Shimamura, T., Ji, H., Minami, Y., Thomas, R.K., Lowell, A.M., Shah, K., Greulich, H., Glatt, K.A., Meyerson, M., Shapiro, G.I., and Wong, K.K. (2006). Non-small-cell lung cancer and Ba/F3 transformed cells harboring the ERBB2 G776insV_G/C mutation are sensitive to the dual-specific epidermal growth factor receptor and ERBB2 inhibitor HKI-272. Cancer Res. *66*, 6487–6491.

Vignot, S., Faivre, S., Aguirre, D., and Raymond, E. (2005). mTOR-targeted therapy of cancer with rapamycin derivatives. Ann. Oncol. *16*, 525–537.

Vogt, P.K. (2001). PI 3-kinase, mTOR, protein synthesis and cancer. Trends Mol. Med. *7*, 482–484.

Zhang, X., Gureasko, J., Shen, K., Cole, P.A., and Kuriyan, J. (2006). An allosteric mechanism for activation of the kinase domain of epidermal growth factor receptor. Cell *125*, 1137–1149.